Estuarine, Coastal and Shelf Science 200 (2018) 324–334

Contents lists available at ScienceDirect

Estuarine, Coastal and Shelf Science

journal homepage: www.elsevier.com/locate/ecss

Geospatial analysis of creeks evolution in the Indus Delta, Pakistan using multi sensor satellite data

Muhammad Wajid Ijaz [a, b, *], Rasool Bux Mahar [a], Altaf Ali Siyal [a, c], Muhammad Naveed Anjum [d]

[a] U. S. -Pakistan Centers for Advanced Studies in Water, Mehran University of Engineering and Technology, Jamshoro, 76062, Sindh, Pakistan
[b] Environmental Protection Agency, Lahore, 54000, Punjab, Pakistan
[c] Department of Land and Water Management, Sindh Agriculture University, Tandojam, 70060, Sindh, Pakistan
[d] Division of Hydrology Water-Land Resources in Cold and Arid Regions, Northwest Institute of Eco-Environment and Resources, Chinese Academy of Sciences, Lanzhou, Gansu, 730000, China

ARTICLE INFO

Article history:
Received 20 July 2017
Received in revised form
13 November 2017
Accepted 22 November 2017
Available online 23 November 2017

Keywords:
Satellite imagery
Coastal morphology
Sindh coast
Mangrove

ABSTRACT

Sea level rise (SLR) in response to looming climate change is being considered as a major impediment to coastal areas. Acute wave activities and tidal propagations of semi-diurnal to mixed type are impairing the morphology of the Indus Delta in Pakistan. In this study a synthetic approach has been adopted using multi sensor satellite and ground data in order to integrate the individual effect of topography, oceanic activities and vegetative canopy for deduction of a synergic impact over the morphology of the Indus Delta creeks system from 1972 to 2017. Geomorphologic anomalies in the planform of fourteen major creeks were explored. Spatiotemporal variations suggested that a substantial amount of the delta alluvium had been engulfed by the Arabian Sea. On average, the creeks located on the right side of the Indus River were relatively less wide (3.9 km) than those of on the left side (5.2 km). Zonal statistics calculated with topographic position index (TPI) enabled to understand the tide induced inundation extents. The mangrove canopy on the right side was found greater, which is why tidal basins on that side experienced less erosive activities. Thus, it could be maintained that the coastal sedimentary processes may be monitored effectively with the remotely sensed data and temporal pattern of changes can be quantified for future planning and mitigation of adverse effects.

© 2017 Elsevier Ltd. All rights reserved.

1. Introduction

The interaction between land and oceans has always been of dynamic nature (Sarmiento et al., 2016). Coastal areas have been severely affected by the ongoing warming of the global climate in the form of mean sea level rise and extensive erosion due to more frequently occurring storms and cyclones. The earth is experiencing continuous warming since 1980 (IPCC, 2013). Glacial retreat and thermal expansion of the sea water in response to global warming is rendering undesirable eustatic sea level rise. This phenomenon has disturbed the so-called equilibrium between land and oceans. Evidences across the globe suggest that sea level rise (SLR) has accelerated at a notable rate and low-lying settlements in coastal systems are under a great threat of calamities (Spencer et al., 2016; Leonard et al., 2017; Parekh et al., 2017). Ecological and geomorphological transitions along their interfaces have become more frequent over short to the long timescales (Ryu et al., 2008).

Basically, the spatial arrangement of the wetlands and topographic orientation of the tidal basins determine their tidal hydrology and inundation patterns (Li et al., 2014; Liu et al., 2013; Kang and Ding, 2013) and correspondingly dominance of flood or ebb tides determine the channel morphology (Tambroni et al., 2017). Whilst, physiographic features of the landscape and contextual placement of the flora plays a pivotal role in the geomorphologic evolution of the coastal systems (Daidu et al., 2013). Minimization of uncertainties in understanding and prediction of their mutual interactions is a core issue in coastal management (Grosholz, 2002; Cash and Moser, 2000; Dalyander et al., 2016).

Indus Delta falls into the category of those deltas of the world

* Corresponding author. U. S. -Pakistan Centers for Advanced Studies in Water, Mehran University of Engineering and Technology, Jamshoro, 76062, Sindh, Pakistan.
E-mail addresses: wajidijaz331@gmail.com (M.W. Ijaz), rb.mahar@faculty.muet.edu.pk (R.B. Mahar), aasiyal.uspcasw@faculty.muet.edu.pk (A.A. Siyal), naveedwre@lzb.ac.cn (M.N. Anjum).

https://doi.org/10.1016/j.ecss.2017.11.025
0272-7714/© 2017 Elsevier Ltd. All rights reserved.

which are more vulnerable to SLR (UNEP-DHI and UNEP, 2016). Heavy fluvial fluxes of the Indus River originating from the Himalayan range used to drain into the Arabian Sea through numerous natural waterways. However, since 1861 until now the number of natural waterways has decreased from 17 to 1 due to artificial impoundments, extensive upstream abstractions, and confinement of the river course within man-made levees (Syvitski et al., 2013). Such anthropogenic perturbations have significantly weakened its natural regimes, and consequently, oceanic activities along the Sindh coast are exacerbating the morphological setting of the delta alluvium through unprecedented erosion in its creeks network (Inam et al., 2007; Mahar, 2010).

Geographically, the Indus River bisects the Lower Indus Basin in the Sindh province of Pakistan into two major zones. The right (western) side is comprised of irrigated and dry lands bounded within the right bank of the river and Khirther mountains of the Sulaiman range while the left (eastern) side is also irrigated plain ranging from the left bank to the Thar desert. Both sides, connect with the Indus delta that borders the Sindh coast in the south of the province. Topographically, the terrain of the province is flat where nearly one-fifth of the canal command areas face major issues of waterlogging and soil salinity (SIDA, 2013). Rehabilitation projects are underway to mitigate the problems for sustainable agriculture that includes (1) the Left Bank Outfall Drain (LBOD) which was completed in 1997 for disposal of agricultural and industrial effluents into the Arabian sea, revival of natural waterways, mangroves plantation, rehabilitation of wetlands, and forest plantation with drainage water, (2) the Right Bank Outfall Drain (RBOD) is a project of disposal of effluents from province Baluchistan to the sea through province Sindh and more than 50% of its construction work is completed.

Wetlands ecosystem of the Indus Delta supports a wide range of biodiversity like plants, birds, fish, wildlife and other aquatic life of economic value for locals (Mitsch and Gosselink, 2000). In the coastal and deltaic plains of Pakistan, more than 100 wetlands exist and among them 90% fall on the left side. However, the left side is older than the other, and 6 out of 19 declared Ramsar wetlands of the country also lie on that side (SIDA, 2013; Rahman, 1960). The largest natural lake in Pakistan, namely Manchar lake and a protected game sanctuary as well as Ramser site, namely Haleji lake exists on the right side. In a comparative study on floral species assessment of both sides, Khatoon and Akbar (2008) found that biodiversity on the right side was greater than the other side.

The Indus River presently drains into the Khobar Creek, which is connected with the Arabian Sea. A study by Tabrez et al. (2013) revealed that suspended sediment load at the Kotri barrage (locating about 250 km upstream from the river mouth) during peak flows in 2003 was 65–92 ppm (parts per million) while at the Khobar Creek mouth, where sediment of fluvial and oceanic origin interact, was about 500 ppm. A study by Saleem et al. (2014) determined that suspended sediment concentration in the Hajamro Creek during the northeast monsoon period of 2013 on the right side was 40–100 ppm in a complete tidal cycle while National Institute of Oceanography, Pakistan (National Institute of Oceanography, 1995) reported that in the Shah Samando Creek on the left side it was about 1298 ppm in 1994. The physical characteristics of the soil on the right side were ranging from silt to sand while on the other side was ranging from clay to silt, predominantly (Tabrez et al., 2013). Thus, a distinct difference in the landscape, suspended sediment load and ecological features on the both sides of the Indus Delta motivated us to analyze and compare the eco-geomorphological evolution of the right and left sides over the same timeline.

Various methods, such as field surveys, mathematical modeling, and remote sensing techniques have been used by researchers for revealing the underlying processes and their subsequent impacts over coastal sedimentary systems. However, remote sensing, especially the application of satellite images and retrieval of geospatial information has become an indispensable source of monitoring the coastal systems because it has fewer constraints of financial and human resources (Richards and Jia, 2006; Gade et al., 2014; Harrison et al., 2017; Liu and Mason, 2016).

The literature review shows that most of the research results are limited to the assessment of morphologic degradation on reach- or basin-scale and on temporal scale from short to long timelines but the present study aimed to 1) examine the evolution of tidal creeks network in the Indus Delta, Pakistan, and 2) investigate the potential causes of differential morphologic response of either side of the delta. A large number of geomorphologic parameters along with adequate field observations have been analyzed for determination of more vulnerable creeks and understanding the potential reasons for their anomalous evolution. This evidence-based assessment would help the coastal managers and ecologists for interpretation of land degradation from multi sensor digital imageries and strengthen the integrated coastal zone management (ICZM) plans against the looming threat of climate change and sea level rise.

2. Methodology

2.1. Study area

Sindh coast, one of the most significant offshore areas of the northern Indian Ocean, starts from Karachi and spans up to the Sir Creek near the international border of Pakistan and India (Fig. 1). It looks like an arc shape which is the basically the lower boundary of the fan-shaped Indus Delta. Makran coast of Pakistan in the northwest and Gujrat coast of India in the Southeast also share their boundaries with this coast. After flow regulations and river training works along the main Indus River, the mouths of the creeks were predominantly exposed to oceanic activities that is why the quality and quantity of the adjoining lands are deteriorating perpetually. Fourteen major creeks and many other minor creeks form a naturally carved dendritic network of waterways in the tidal flats (Fig. 1) of the Indus Delta.

This creeks network stretches about 180 km along the Sindh coast and on average it extends longitudinally up to 32 km landward. Physiographically, the tidal flats are composed of tidal cover plain with coarse-textured sediments and gradation approaches to finer sediments landward (WAPDA, 1966). Semi-diurnal to mix types of tides with tidal range 3.5–5.0 m intrude into the creeks (Waheed-uz-Zaman and Saif, 2014).

2.2. Dataset

The dataset used in this study along with software packages used for processing, extraction of required information and its presentation are described in Table 1. The software packages protected under license were acquired from Geographical Information System (GIS) section of the U. S. -Pakistan Centers for Advanced Studies in Water (http://water.muet.edu.pk/), Pakistan and all of the data was graciously shared by the respective agency free of cost, which is duly acknowledged in the forthcoming sections. The width of any water channel, i.e. river or creek is more sensitive to the prevailing stage of water at the acquisition time of aerial or satellite images in a planimetric analysis. Although, identical tidal levels and image acquisition time of any satellite coincide rarely. Therefore, utmost care was taken while the selection of the satellite images used in this study. It was considered to undertake the analysis on similar upstream (river) and downstream (tidal) conditions so that

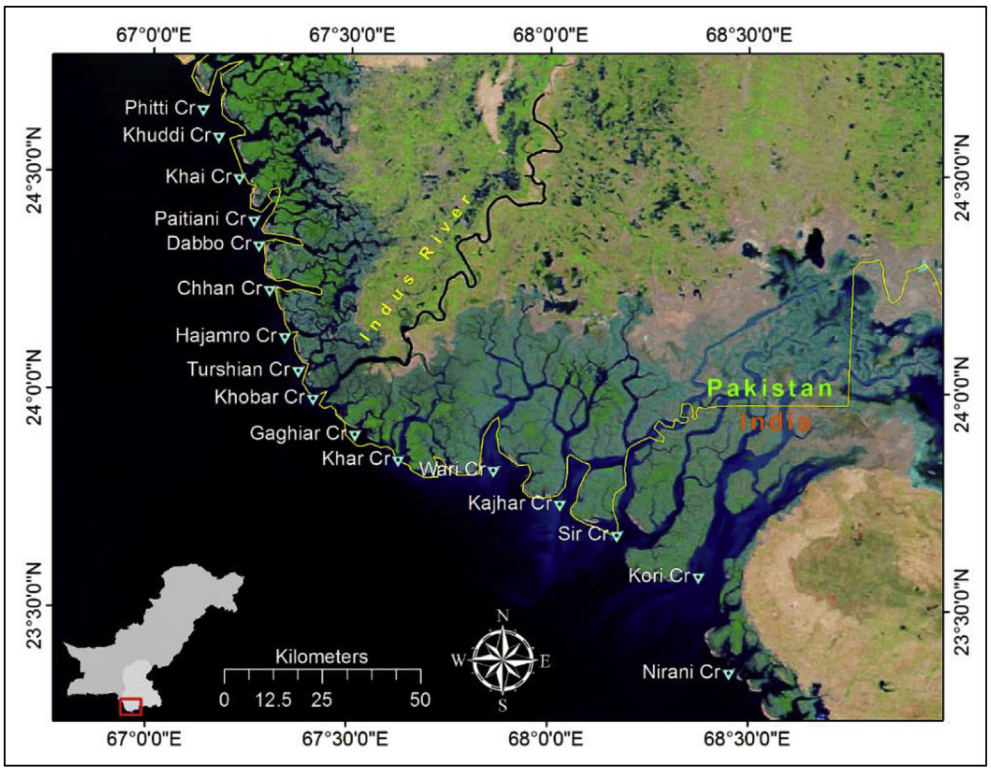

Fig. 1. Location of study area showing spatial distribution of major creeks in the Indus Delta.

Table 1
Description of data sets with necessary meta-information.

Data Set	Description	Spatial and Temporal Resolution					Source	Processing Software
		Pixel Size	Date of Acquisition	Time of Acquisition (UTC)	River Discharge at the time of Image Acquisition (m3/s)[b]	Tidal Level at the time of Image Acquisition[c]		
Satellite Data	Landsat multi-spectral imageries	60 m	15-10-1972	05:26	0	1.84 m	United States Geological Survey (http://glovis.usgs.gov/)	ArcMap 10.3.1 and Google Earth Pro
		30 m	15-02-1995	05:08	0	2.53 m		
		30 m	11-02-2017	05:57	0	2.57 m		
Hydrologic Data[a]	Annual volume	1970–2015					Irrigation & Power Department (I & PD), Sindh, Pakistan	Origin Pro 2016 and Microsoft Excel 2013
	Highest flood peak	1901–2014 at Kotri barrage					Federal Flood Commission, Pakistan	
Oceanographic Data	Relative mean sea level	1916–2014					Sea Level Center of the University of Hawaii, USA (Caldwell et al., 2015) http://uhslc.soest.hawaii.edu/datainfo/	
	Mean tidal level	2010–2017					Tides 4 Fishing http://www.tides4fishing.com/	
Topographic Data	Digital Elevation Model	C-band SRTM Version 4 2001 (30 m)					United States Geological Survey (http://earthexplorer.usgs.gov/)	Planlauf/TERRIAN, ArcMap 10.3.1,
	Surface contour map	1:750,000 scale map of 1966 1.524 m (5 ft) interval					Water And Power Development Authority (WAPDA), Pakistan (WAPDA, 1966)	Global Mapper 13 and ArcMap 10.3.1

[a] Unpublished.
[b] I&PD, Sindh & WAPDA.
[c] UK Hydrographic Office for Karachi station.

the results may be discussed on equal and comparable boundary conditions (Table 1). Thus, all the images under question were acquired during high tide and zero flow of the Indus River from upstream.

Moreover, all the software packages and geospatial algorithms in Spatial Analyst Tool of ArcMap 10.3.1 were executed on HP Z400 desktop workstation and Core i7 6th Generation Dell laptop having extended Graphic Processing Unit (GPU). Topographic map of the study area was first scanned and then georeferenced for further process. Ground truthing for pixel training of multispectral imagery

with georeferenced points was done during field surveys.

2.3. Data processing and methods

Morphologic features of the creeks network, i.e., channel planform (2D), centerline, water edge and coastal boundary were extracted from the multispectral satellite imageries. Satellite images contain plenty of information in terms of reflectance value assigned to each pixel of the scene which was used in this study for extraction of the feature of interest, e.g., water and vegetation etc (Frazier and Kenneth, 2000). Density slicing is an image processing technique which bifurcates the information of a single band into desired and background feature classes, e.g., water and non-water classes (Ijaz et al., 2017). In this method value of reflectance of water pixels from various points in the image are collected through a 'point shape file' and from those values, a range of minimum to maximum values of reflectance was established. In the next step, all the pixels falling within that defined range were separated using 'Raster Calculator' in Map Algebra of Spatial Analyst Tool executed in ArcMap 10.3.1. Band 7 of Multispectral Scanner (MSS) of Landsat mission was used to separate the pixels representing the water class from the rest of the pixels. Density slicing method was only used for the image of the year 1972 because band indices method was not producing acceptable results for those years. One of the band indices methods is Normalized Difference Water Index (NDWI), which offers relative procedural ease and nowadays being widely used for detection of water bodies and channel planform. It was used for Landsat satellite images of Thematic Mapper (TM) and Operational Land Imager (OLI) sensors for the years of 1995 and 2017, respectively using Equation (1) (Ijaz et al., 2017; Isikdogan et al., 2015).

$$\text{NDWI} = \frac{\text{Green} - \text{NIR}}{\text{Green} + \text{NIR}} \quad (1)$$

Then, the classified raster images were converted into 'polygon shape file' for turning the channel planform into a vector shape. Through on-screen digitization, the center line of each creek channel was drawn within extracted bank lines. From the final planform of each year, the top width at designated transects was measured perpendicular to the centerline. 'Mouth' is an opening section from where deltaic plain connects with the sea, 'Middle' transect is a section which lies in the center of the entire length of a creek channel, and 'Tail' is last section landward from where a creek ends (Fig. 2).

Channel sinuosity (S_e) of meandering tidal creeks was computed using Equation (2):

$$\text{Channel Sinuosity}(S_e) = \frac{\text{Meandering Length}}{\text{Valley Length}} \quad (2)$$

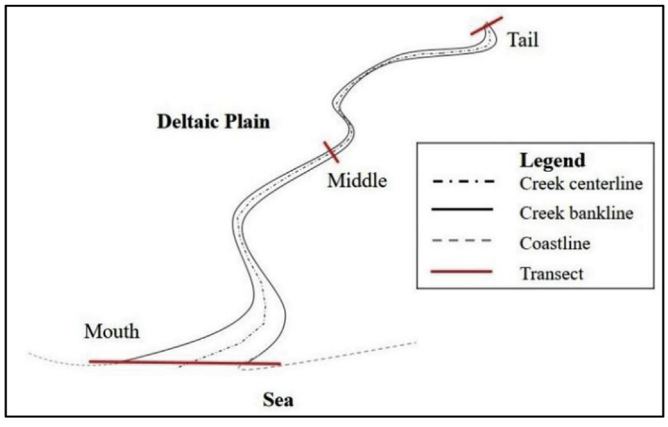

Fig. 2. Schematic planform of a creek channel along with transects from where temporal analysis of top width was undertaken.

Topographic information (3D) of tidal flats was retrieved from Digital Elevation Model (DEM) recorded with the Spaceborne Imaging Radar band-C (SIR-C) of Shuttle Radar Topography Mission (SRTM) and interpreted with survey based 1.524 m spacing contour map of the study area (WAPDA, 1966).

Topographic position index (*TPI*) is an automatic land classification method in which the elevation of each cell in the digital elevation model is compared with respect to the user-defined neighborhood around every cell (De Reu et al., 2011; Mokarram et al., 2015; De Reu et al., 2013). In order to determine the ruggedness of terrain, *TPI* was computed using 30 cells by 30 cells neighborhood size with the rectangular shape by implementing the Zonal Statistics algorithm in ArcMap 10.3.1 environment (Jenness, 2006; Weiss, 2001) as follows:

$$\text{TPI} = Z_o - \frac{\sum_{1-n} Z_n}{n} \quad (3)$$

Where Z_o is the elevation of the point under consideration, Z_n is an nth number of surrounding points. Continuous *TPI* values were discretized with thresholding technique in predefined classes of slope positions. Using topographic analysis, low relief coastal terrain was subdivided into low, mild and high slope areas. Point-based ground-truthing survey of the coastal areas was done using Handheld GARMIN GPSMAP-64 device for field data collection (Wang et al., 2003). During field surveys from July 2016 to April 2017, coordinates of bare land, mangrove clusters (dense and sparse) and intertidal areas were collected on a boat from various creeks on both sides of the delta (exact locations exhibited in Fig. 10). On the basis of field data of land-use, the reflectance of multispectral satellite images was trained on a pixel scale (Khatoon and Akbar, 2008). Pixel-based supervised classification using maximum likelihood algorithm was used to quantify the areas under mangrove canopy (Ijaz et al., 2017). The oceanographic analysis was undertaken with statistical trend analysis.

3. Results and discussion

3.1. Spatio-temporal width variations

The top width of the creeks network was measured from the planform. Measurements of 'mouth' transect revealed that top width of creeks existing on the right side of the Indus River was relatively uniform in 1972, but afterward they started following a spatially decreasing trend from the rightmost the Phitti Creek up to the Hajamro Creek (Fig. 3). Reduction in the 'mouth' width was also noticed in the Chhan and Hajamro Creeks, existing adjacent to the Indus River. During 1972 to 2017, these two creeks have got narrowed 9% and 7%, respectively. Similarly, 'mouth' of the Turshian Creek immediate to the Indus River on the left side also reduced the width 17%.

Another, the Wari Creek got narrowed in the result of deposition of alluvium. Generally, the creeks on the left side are wider from the Turshian Creek up to Sir Creek. Mean values of the 'mouth' width averaged on the right (3884.065 m) and left (5222.952 m) sides of the delta showed that the 'mouths' of the creeks on the left side are wider but the magnitude of increment in width is higher at the right side (Table 2). Modification of the creek mouth is a self-adjusting but a complex morphological process which depends upon various factors like hydrologic, oceanographic, geologic and

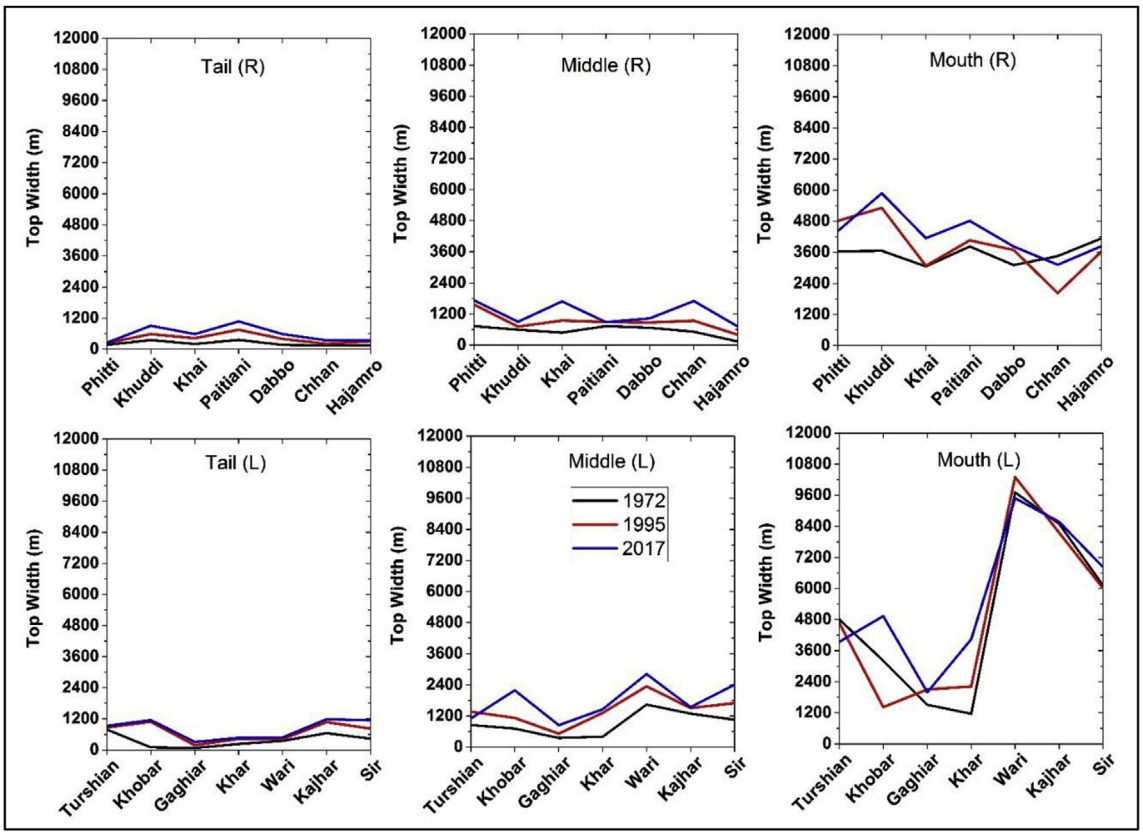

Fig. 3. Temporal variations in the top width of the creeks network at the mouth, middle and tail transect over the longitudinal scale. '*L*' and '*R*' express the left and right sides, respectively.

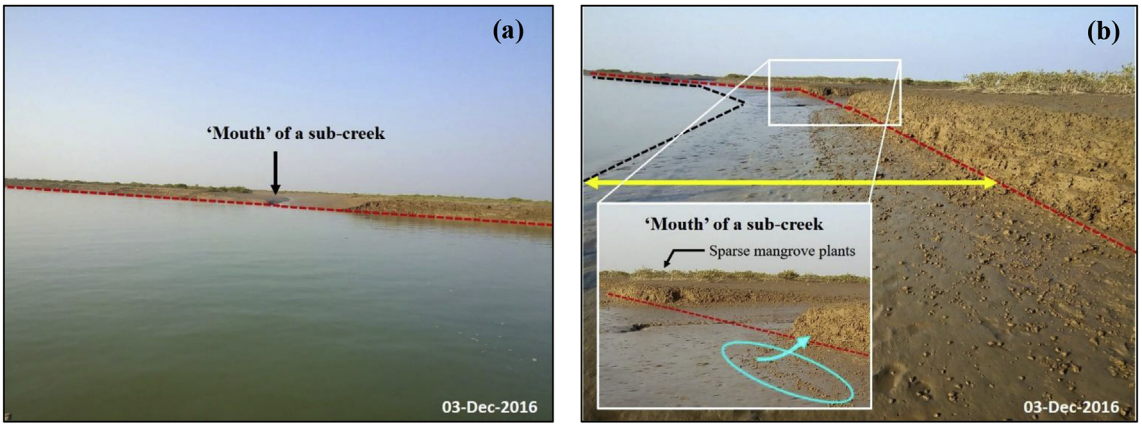

Fig. 4. Exposure of channel geometry of a sub-creek existing in intertidal zone between the Hajamro and Turshian Creek during ebb tide (a) Channel bank observed on a boat during high water stage (marked with red dotted line), (b) Recession of tidal stage over flatter mud flats and evacuated land between high and receding stage (shown with yellow arrow) and inset an example of alignment of small lumps of clayey soil (sky blow circle) which have deposited over the ramp and their gradual deposition may result narrowing of mouth transect. (For interpretation of the references to colour in this figure legend, the reader is referred to the web version of this article.)

metrologic settings (Stive and Wang, 2003). It is worth mentioning here that the creeks having a physical connection with the Indus River predominantly exhibited a narrowing trend at mouth transect, which is more likely that the supply of fluvial sediments and enhanced deposition along the banks. As the detection of mouth and other two transects and their subsequent width measurements were solely based upon the segregation of water and non-water pixels in the satellite images of respective years that is why the width of the channel at the time of high tidal level was presumably accepted as the maximum width of the channel (See Fig. 4).

'Middle' and 'tail' transects of creeks on both sides have expanded dramatically during the year 1972–2017. The highest expansion was observed on the right side of the Indus River that was in the 'middle' transects of Chhan and Hajamro Creek as 227% and 408%, respectively. Similarly, 'middle' transects of Khobar and Khar Creeks on the left side got wider 206% and 246%, respectively.

However, top width of 'tail' transect of the Khobar Creek on the left side expanded 1101% that is extraordinary and highest

Table 2
Statistically averaged top width of the channel planforms and level of coefficient of determination for simulation function.

Cr. No.		Name	Averaged Top Width (m)				R^2 of Exp. Function
			Mouth	Middle	Tail	Averaged	
1	Right Side	Phitti	4292.577	1339.513	219.553	1950.548	0.858
2		Khuddi	4953.930	733.136	613.963	2100.343	0.866
3		Khai	3427.810	1037.597	404.273	1623.227	0.994
4		Paitiani	4234.473	835.196	728.446	1932.706	0.870
5		Dabbo	3541.490	857.573	381.243	1593.436	0.962
6		Chhan	2866.800	1052.280	232.640	1383.907	0.999
7		Hajamro	3871.373	416.443	263.676	1517.164	0.706
		Mean	3884.065	895.962	406.256	1728.761	
		SD	±682.494	±289.496	±197.022	±265.205	
8	Left Side	Turshian	4471.12	1105.503	859.396	2145.340	0.774
9		Khobar	3189.657	1342.550	777.616	1769.941	0.955
10		Gaghiar	1869.003	570.030	184.686	874.573	0.907
11		Khar	2474.433	1056.887	373.063	1301.461	0.978
12		Wari	9832.370	2265.533	417.603	4171.836	0.997
13		Kajhar	8406.963	1446.883	967.060	3606.969	0.981
14		Sir	6317.12	1716.897	800.443	2944.820	0.993
		Mean	5222.952	1357.755	625.696	2402.134	
		SD	±3057.361	±537.879	±296.192	±1217.135	

expansion in any transect from 1972 to 2017. One of the major reasons for this extraordinary expansion was variation in the magnitude of the river floods. Kotri barrage is the last flow regulation structure erected across the Indus River at approximately 250 km upstream of the river mouth. A thorough investigation of this section (Figs. 5 & 6C) revealed that after 1976 to onwards 'very high' level floods below Kotri barrage resulted in the opening of the Khobar Creek 'tail' and major proportionate of the river flows started flowing through the Khobar Creek instead of the Turshian Creek in result of channel switching. Overall, it was noticed that 'tail' transects of creeks existing on both sides were enlarging more rapidly than the other sections.

3.2. Longitudinal trend analysis

Longitudinal variation in the width of each creek was also assessed through trend analysis. It was observed that the top width of creek channels followed a landward decreasing trend. The converging banks of the creeks network over longitudinal distance were fairly simulated with best-fit exponential function. The values of the coefficient of correlation on the right side varied from 0.70 to 0.99 while this range was 0.77–0.99 on the left side (Table 2). Except for the Turshian Creek, the width of all the remaining creeks on the left side was decreasing exponentially, but creeks on the right side exhibited mixed, i.e., good ($0.8 > R^2 > 0.7$) to significant ($R^2 > 0.8$) level of the correlation. Like spatiotemporal width

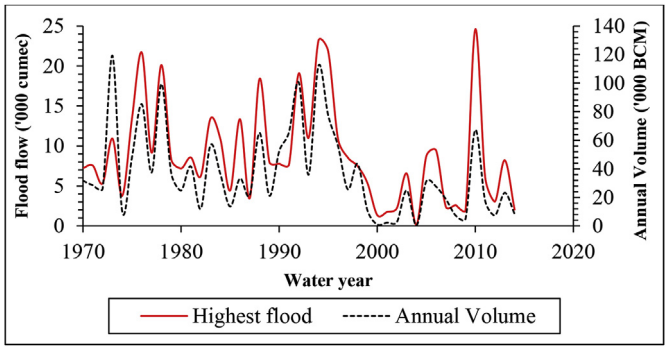

Fig. 5. Variations in highest annual floods and average annual volume of water resealed from the Kotri Barrage to the Indus Delta.

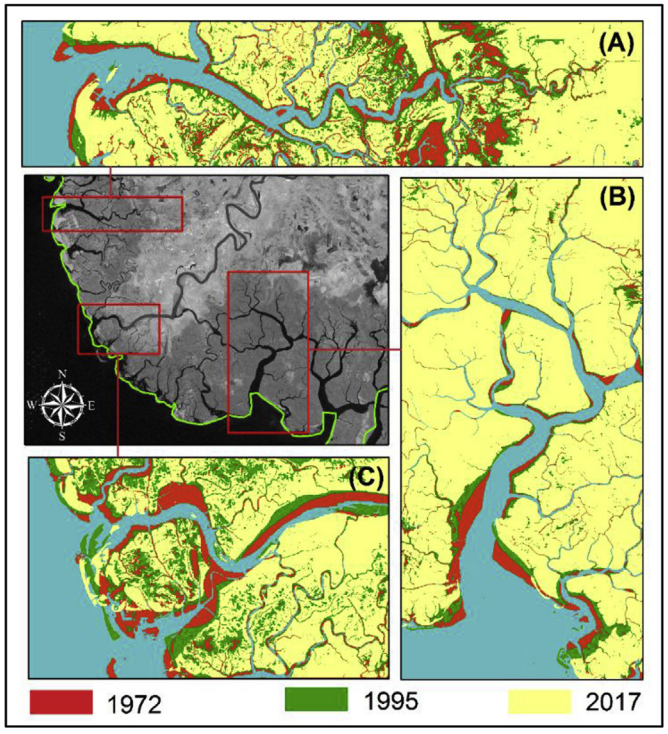

Fig. 6. Creeks evolution in Indus delta **(a)** temporal expansion of the 'tail' transect at Dabbo Creek, **(b)** widening of the 'mouth' transect of Wari Creek, and **(c)** diversion of the flow path of the Indus River from the Turshian to Khobar Creek.

variations, the strength of the exponential function of longitudinal width also decreases near the Indus River but it improves as observations were made near the northwestern (right) and the southeastern (left) flanges of the delta.

3.3. Length and sinuosity

Length and sinuosity of the creeks are differently distributed along the coast of Sindh, Pakistan. From Fig. 7, it is shown that the sinuosity line of the creeks on the right side is bimodal while unimodal on the left side. Average sinuosity of the creeks on the right side is 1.417 and on the left side is 1.248 which is similar to the

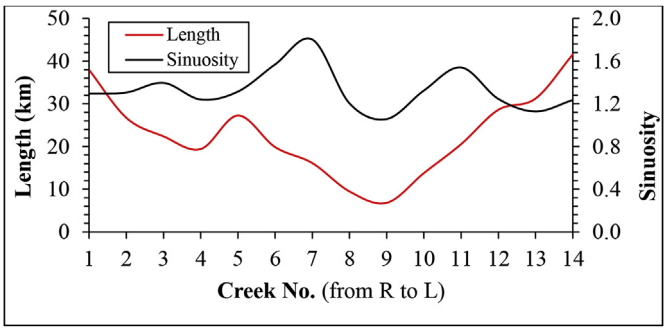

Fig. 7. Spatial variation in sinuosity and the corresponding length of each creek.

case of the length of these creeks. The average length of the creeks on the right side is 33.62 km while it is 27.22 km on the left side. However, spatial variations in the length of the creeks along the coastline follow the similar trend on both sides of the delta, i.e., the curve defining the longitudinal length of the creeks converges near the Indus River and ascends towards the right and left lobes of the delta (Fig. 7). Nevertheless, Khobar and Sir Creeks are the shortest and longest creeks among all others. Both are situated, coincidentally, on the left side having length 7.19 km and 51.29 km, respectively.

The natural funnel-shaped geometry of the creeks is probably due to the phenomenon of morphological equilibrium analogous to the entropy principle of thermodynamics (Kleidon and Renner, 2013; Kleidon et al., 2014). Savenije (2005, 2015) maintained that the 'mouth' of coastal plain estuaries interact with full tidal range but the subsequent tidal energy in the creek channel is dissipated due to channel friction, as it propagates further landward and ultimately tide gets damped.

3.4. Topographic analysis

Two lateral transects (from left to right) at each side of the delta were drawn for assessment of topographic variations. Altimetric

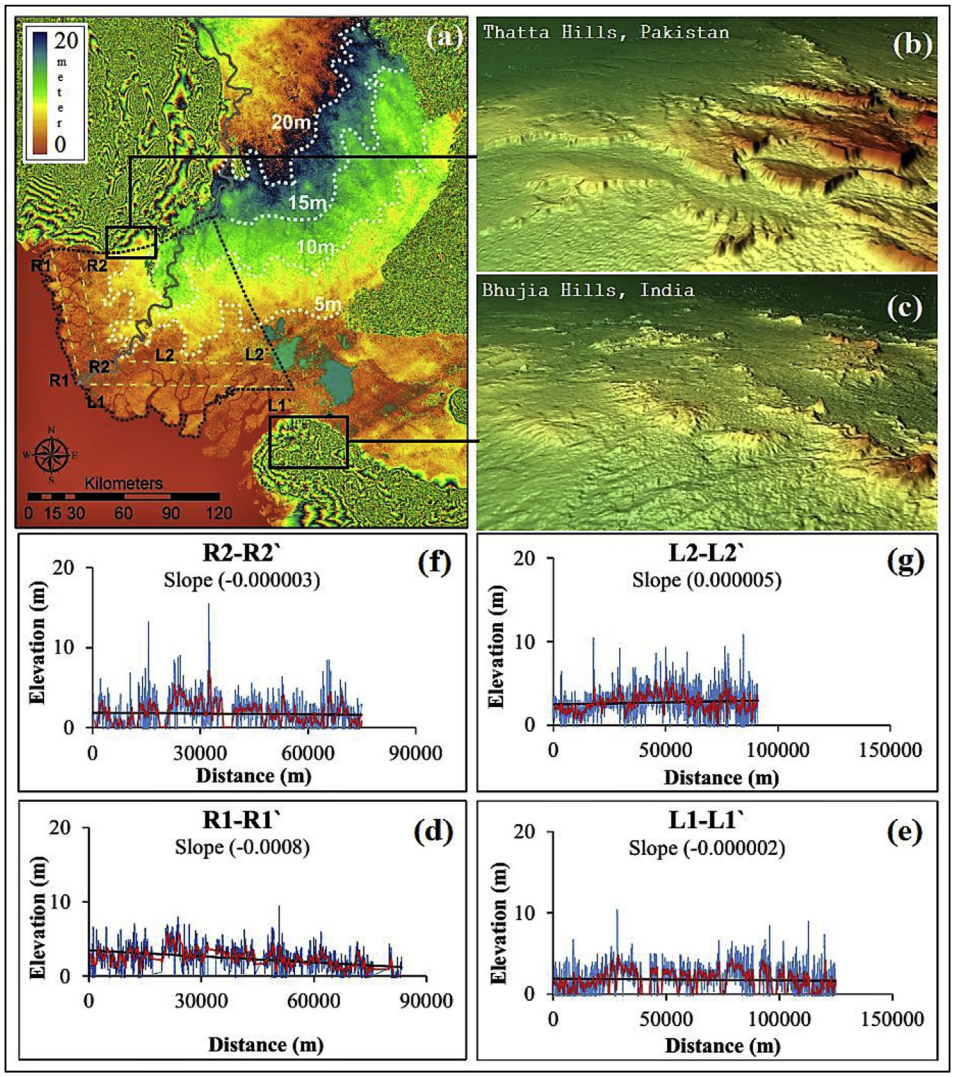

Fig. 8. Topographic configuration of the delta alluvium and incised creek channels **(a)** 5 m contours drawn over SRTM-DEM of 30 × 30 m with color change at every 5 m vertical elevation and color repetition at every 20 m **(b)** situation of Thatta Hills, an extension of Khirther range of mountains which joins uplift zone **(c)** Bhujia hills in Indian territory adjacent to Rann of Kutch, an active fault zone in the south-eastern side **(d-f)** elevation lines from left to right showing orientation and slopes (shown with black linear trend line and slope of the line found from trend line equation) of the right and left lobes of the delta in lateral and longitudinal direction. (For interpretation of the references to colour in this figure legend, the reader is referred to the web version of this article.)

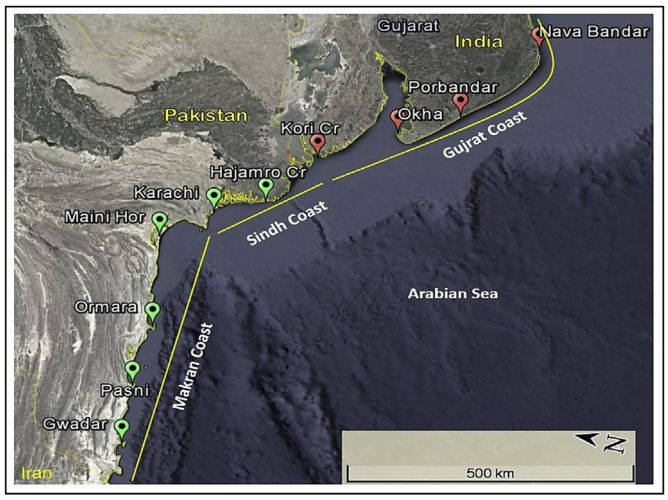

Fig. 9. Spatial distribution of tidal stations (Green: Pakistani and Red: Indian) along the Makran, Sindh and Gujrat coasts (Image: Google Earth Pro). (For interpretation of the references to colour in this figure legend, the reader is referred to the web version of this article.)

Table 3
Topographic Position Index (TPI) 30 × 30 arc-sec of tidal flats on the right and left lobes of the Indus Delta.

Category	TPI	Right Side (%)	Left Side (%)
Lower slope	0.00–0.25	8.62	6.05
Flat area/Mild slope	0.25–0.50	54.10	52.28
High Slope	0.50–1.00	37.28	41.68

view of transects R_1-R_1' and L_1-L_1' near the tidal inlets showed that the terrain of tidal flats inclines from southwestern to the southeastern side with a negative slope of 0.0008 m/m and 0.000002 m/m, respectively (Fig. 8 (d&e)). However, the terrain, on both sides, near tails of the creeks is not identically inclined. The profiles of elevation along lateral transect R_2-R_2' and L_2-L_2' demonstrate that the slope on the right side was −0.000003 m/m and on the left side was 0.000005 m/m. It could be deduced from the lateral topographical analysis that the left and right lobes of the delta are placed in such a way that the terrain of the tidal flats makes a concave dip over whose bed the Indus River is carved. Similarly, it could also be considered that due to relatively larger inclination on the right side, the low relief area (below 5 m contour) was lesser as compared to the left side that is why the effect of sea intrusion was less pronounced on the right side. This substantial finding could also be witnessed from the difference in the averaged top width of the creeks on both sides (Table 2).

Zonal statistics of the topography were computed for determination of inherent spatial variation in the slope of each gridded cell of the terrain. Based on quantitative analysis of predefined categories of topographic position index (TPI), it was observed that proportionate of the mild to high slope areas on the left side was relatively larger than that of the right side (Table 3). It infers that the erosive effect of the tides on the left side was more vigorous which could be substantiated by landward elongation of the left side creeks.

It is also worth mentioning that the left lobe of Indus Delta is facing subsidence problems due to ongoing extensive mining activities for exploration of petrochemical products (Rahman, 1960; Bendick et al., 2001; Biswas, 2005; Jorgensen et al., 1993). Another potential cause of the subsidence was reported by Shroder (2002) who maintained that the existence of an active tectonic fault zone near the edge of the Rann of Kutch (Fig. 8c) had been rendering the subsidence effects over the southeastern side and consequently exposure of that part to the tidal effect is increasing.

3.5. Oceanographic analysis

Tidal flats along the Sindh coast border with the deltaic plain in a transgressive form. Sediment depositional features keep emerging under semi-diurnal to the mixed type of tides along the coast. Statistical analysis of the oceanographic data from 1916 to 2014 at Karachi station revealed that the mean sea level (MSL) along the coast was observing a rising trend, also reported by Woodworth et al. (2009). However, the increase in MSL since 1980 was distinctively sharp (Fig. 10a). Mean tidal level along the entire coastal stretch (whole Pakistani coast to some part of Indian coast) ranges from 1.42 m at Ormara to 2.18 m at Okha station. It is evident from the spatial analysis that the mean tidal level increases towards the southeastern side (Fig. 10b) which is identical to the findings of Waheed-uz-Zaman & Saif (2014), and NIO (1995), who reported that the tidal range had been varying from 2 m to 5 m along the Karachi coast (Meso tidal, 2–4 m) up to Sir Creek (macro-tidal, >4 m), respectively.

Using a classification model of Boyd et al. (1992), it was found that the left side comprised of mature creeks with larger inlets and wider middle transects collectively producing the embayment effect, while on the right side the coast was relatively linear with shorter creeks, which demonstrates that the left side had been experiencing wave dominated and the right side had undergone through the tide-dominated processes.

3.6. Vegetative cover

Avicennia marina is one of the major species of mangroves in the Indus Delta which covers more than 95% of the available canopy. A notable temporal trend and spatial distribution of mangrove plantation are tabulated in Table 4. The area under vegetative cover on the right side was remarkably higher than that on the left side. Rise in the mangrove area of the right side was first abrupt then followed by steady trend but that area on the left side was 1) lesser than that on the right side, 2) increased steadily in the beginning but afterward decreased or stuck in an earlier condition.

Biophysical services (wind breaking, strata-binding, sediment trap, hydraulic resistance, nutrients/pollutants uptake and salt tolerance) rendered by a mangrove tree are well recognized as a natural mean of coastal defense. Therefore, the evolution of mangrove canopy on both sides of the delta is quite superposable with the morphological patterns explained earlier herein. An increase in the vegetative cover on the right and left side, also reported by Masood et al. (2015), is an evidence of constructive deliberations made by local government and international agencies like World Bank (WB), Asian Development Bank (ADB), International Union for Conservation of Nature (IUCN), World Wide Fund (WWF) agencies (SIDA, 2013) and natural response of these measures could be actualized from relatively stable morphology of the right side and continuously deteriorating condition on the left side (Fig. 11).

Oceanic activities on the left side were more drastic that is why the survival of the mangroves is uncertain, and resultantly creek channels were widening at a substantial rate. However, the condition on the right side reflects that the oceanic activities on this side are relatively lighter that is why a multiplicative growth of the mangrove canopy was witnessed by the use of satellite imageries and field surveys.

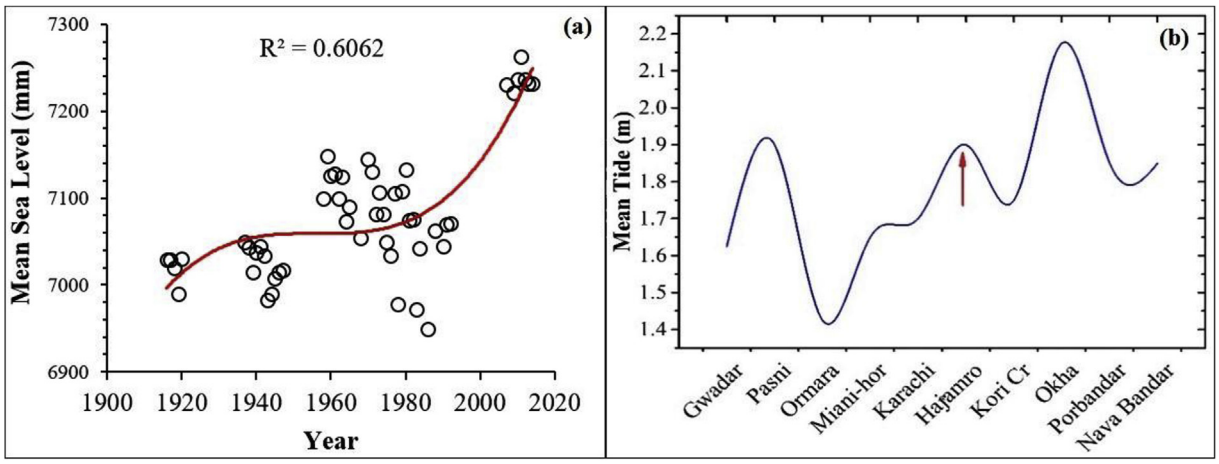

Fig. 10. **(a)** Sea level rise at Karachi station from 1916-2014 with 3rd order polynomial trend line (red color) **(b)** Variation in mean tidal level along the coastal zone as depicted in Fig. 9. (For interpretation of the references to colour in this figure legend, the reader is referred to the web version of this article.)

Table 4
Temporal variation in mangrove canopy in the Indus Delta.

Year	Right Side (ha)		Left Side (ha)	
	ha	%	ha	%
1972	9210.33	4.30	7712.01	1.81
1995	32720.9	15.27	24799.41	5.82
2017	43626.2	20.36	22214.43	5.21

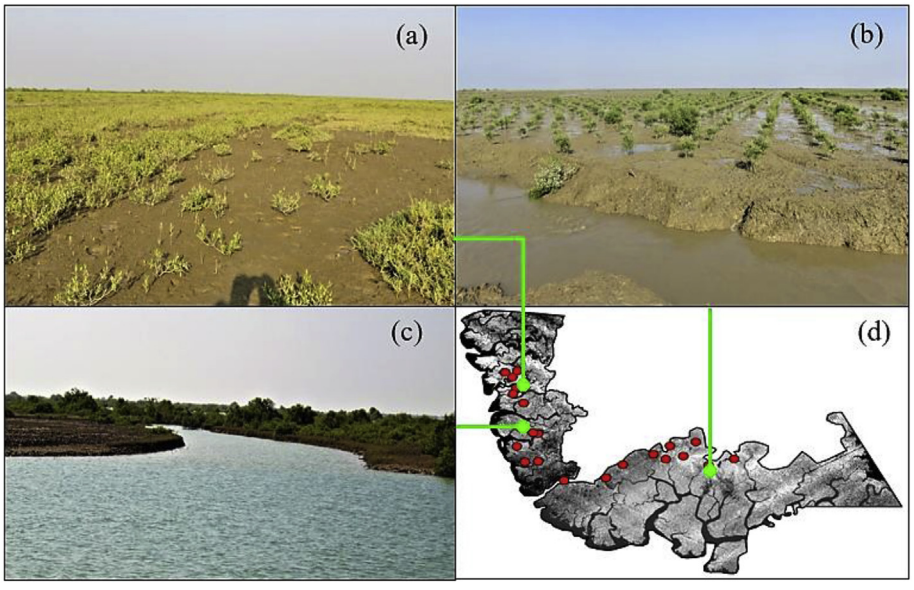

Fig. 11. Ground situation of mangrove canopy **(a)** naturally vegetated mud flates in a scattered pattern, **(b)** planted by local agencies for mitigation of erosive activities of tides, **(c)** inlet/mouth of a typical tidal creek near Keti Bandar, **(d)** geo-referenced ground points (in red color) on both sides of the Indus delta where channel banks and land-use observations were made. (For interpretation of the references to colour in this figure legend, the reader is referred to the web version of this article.)

4. Conclusion

In this study morphological evolution in terms of shortening or widening of the creeks network in the Indus Delta, Pakistan has been evaluated with the use of satellite and field data. On the basis of analysis and the results, following conclusions are drawn:

1. The creeks network is very dynamic in morphologic response to the oceanic activities. The right side of the delta is less affected or more stable than that of the left side. The size of the creeks (in terms of the length and width) on the left side is larger than the right side. Although, fluvial regimes of the Indus River have weakened in terms of its seasonal water and sediment supply but the effect of so far river flows can still be witnessed from relative improved morphologic conditions of the adjacent creeks.
2. Contextual information about the topography combined with spatial variations in tidal features enabled to explore the reasons

behind the differential response of the coastal sedimentary systems existing on both sides of the delta. Banks of the creeks were sharper on the left side because of the prevalence of wave-dominated processes with a higher tidal range. A larger proportionate on the left side below the 5 m contour combined with subsidence effects on the southeastern side produce embayment effect that is why widening and elongation of the creeks is degrading the valuable alluvium of Indus delta more rapidly.

3. Geospatial arrangements of the mangrove canopy proved to have direct control against morphologic deteriorations. More than 20% of the right side area of the delta is occupied by this ecologic feature that is why tidal basins on that side were less prone to oceanic activities, and resultantly erosive action was not so much pronounced.

Hence, it could be maintained that anthropogenic factors are a major determinant of the stability of coastal areas of the Indus Delta. Except for few transects, the major land loss due to expansion in width of the creek channel is depicting that the situation without interventions is drastic and eventually, a heavy cost has to be paid in terms of loss of valuable delta alluvium and subsequent sea intrusion. As the left side is more vulnerable and rich in ecological features consequently, conservation and restoration activities may be initiated from that side on priority. Thus, on the basis of evidence the relevant agencies and the policy makers should reinforce the efforts by planting more mangrove plants, especially along the channel banks as well as over mud flats and construction of levees below the 5 m contour in the lateral direction so that further landward expansion of the creek channels may be curtailed, and remaining delta alluvium may be protected with such structural measures.

Acknowledges

Financial support of the U.S. Agency for International Development, Pakistan and technical assistance by Mr. Arif Naeem, Director Technical, South Region, Water and Power Development Authority, Hyderabad, Pakistan are highly appreciated. Moreover, USGS, United Kingdom Hydrographic Office, and Google Earth are also acknowledged for offering free of cost historic satellite imageries and tidal levels for research purposes.

Appendix A. Supplementary data

Supplementary data related to this article can be found at https://doi.org/10.1016/j.ecss.2017.11.025.

References

Bendick, R., Bilham, R., Fielding, E., Gaur, V.K., Hough, S., Kier, G., Kulkarni, M.N., Martin, S., Mueller, K., Mukul, M., 2001. The January 26, 2001 "Republic Day" Earthquake, India. Seism. Res. Lett. 72 (3), 328–335.

Biswas, S.K., 2005. A review of structure and tectonics of Kachchh basin, western India, with special reference to earthquakes. Curr. Sci. 88 (10), 1592–1600.

Boyd, R., Dalrymple, R., Zaitlin, B., 1992. A, Classification of clastic coastal depositional environments. Sediment. Geol. 80 (3–4), 139–150.

Caldwell, P.C., Merrfield, M.A., Thompson, P.R., 2015. Sea level measured by tide gauges from global oceans — the Joint Archive for Sea Level holdings (NCEI Accession 0019568), Version 5.5. NOAA Natl. Centers Environ. Inf. https://doi.org/10.7289/V5V40S7W.

Cash, D.W., Moser, S.C., 2000. Linking global and local scales: designing dynamic assessment and management processes. Glob. Environ. change 10 (2), 109–120.

Daidu, F., Yuan, W., Min, L., 2013. Classifications, sedimentary features and facies associations of tidal flats. J. Palaeogeogr. 2 (1), 66–80.

Dalyander, P.S., Meyers, M., Mattsson, B., Steyer, G., Godsey, E., McDonald, J., Ford, M., 2016. Use of structured decision-making to explicitly incorporate environmental process understanding in management of coastal restoration projects: case study on barrier islands of the northern Gulf of Mexico. J. Environ. Manag. 183, 497–509.

De Reu, J., Bourgeois, J., De Smedt, P., Zwertvaegher, A., Antrop, M., Bats, M., Crombé, P., 2011. Measuring the relative topographic position of archaeological sites in the landscape, a case study on the Bronze Age barrows in northwest Belgium. J. Archaeol. Sci. 38 (12), 3435–3446.

De Reu, J., Bourgeois, J., Bats, M., Zwertvaegher, A., Gelorini, V., De Smedt, P., Van Meirvenne, M., 2013. Application of the topographic position index to heterogeneous landscapes. Geomorphology 186, 39–49.

Frazier, Paul S., Kenneth, J. Page, 2000. Water body detection and delineation with Landsat TM data. Photogrammetric Eng. remote Sens. 66 (12), 1461–1468.

Gade, M., Melchionna, S., Stelzer, K., Kohlus, J., 2014. Multi-frequency SAR data help improving the monitoring of intertidal flats on the German North Sea coast. Estuar. Coast. Shelf Sci. 140, 32–42.

Grosholz, E., 2002. Ecological and evolutionary consequences of coastal invasions. Trends Ecol. Evol. 17 (1), 22–27.

Harrison, S.R., Bryan, K.R., Mullarney, J.C., 2017. Observations of morphological change at an ebb-tidal delta. Mar. Geol. 385, 131–145.

Ijaz, M.W., Siyal, A.A., Mahar, R.B., Ahmed, W., Anjum, M.N., 2017. Detection of hydromorphologic characteristics of Indus River estuary, Pakistan, using satellite and field data. Arab. J. Sci. Eng. 1–20.

Inam, A., Clift, P.D., Giosan, L., Tabrez, A.R., Tahir, M., Rabbani, M.M., Danish, M., 2007. The geographic, geological and oceanographic setting of the Indus River. Large Rivers Geomorphol. Manag. 333–345.

IPCC, 2013. Working Group I Contribution to the IPCC Fifth Assessment Report Climate Change 2013: the Physical Science Basis, Summary for Policymakers.

Isikdogan, F., Bovik, A., Passalacqua, P., 2015. Automatic channel network extraction from remotely sensed images by singularity analysis. IEEE Geoscience Remote Sens. Lett. 12 (11), 2218–2221.

Jenness, J., 2006. Topographic Position Index (tpi_jen. avx) Extension for ArcView 3. x, v. 1.3 a. Jenness Enterprises. http://www.jennessent.com/arcview/tpi.html.

Jorgensen, D.W., Harvey, M.D., Schumm, S.A., Flam, L., 1993. Morphology and dynamics of the Indus River: implications for the Mohen jo Daro site. In: Shroder Jr., J.F. (Ed.), Himalaya to the Sea. Routledge, London, pp. 228–326.

Kang, Y.Y., Ding, X.R., 2013. Simulation of tidal flat terrain based on landform feature lines of Tidal Basin. In: New Frontiers in Engineering Geology and the Environment. Springer Berlin Heidelberg, pp. 69–73.

Khatoon, S., Akbar, G., 2008. Natural Vegetation Assessment, Indus for All Programme and WWF, Pakistan, pp. 1–131.

Kleidon, A., Renner, M., 2013. Thermodynamic limits of hydrologic cycling within the Earth system: concepts, estimates and implications. Hydrol. Earth Syst. Sci. 17, 2873–2892. https://doi.org/10.5194/hess-17–;2873–2013.

Kleidon, A., Renner, M., Porada, P., 2014. Estimates of the climatological land surface energy and water balance derived from maximum convective power. Hydrol. Earth Syst. Sci. 18, 2201–2218. https://doi.org/10.5194/hess-18–2201-2014.

Leonard, P.B., Sutherland, R.W., Baldwin, R.F., Fedak, D.A., Carnes, R.G., Montgomery, A.P., 2017. Landscape connectivity losses due to sea level rise and land use change. Anim. Conserv. 20 (1), 80–90.

Li, Z., Heygster, G., Notholt, J., 2014. Intertidal topographic maps and morphological changes in the German Wadden sea between 1996, 1999 and 2006, 2009 from the waterline method and SAR images. IEEE. J. Sel. Top. Appl. Earth Obs. Remote Sens. 7 (8), 3210–3224.

Liu, Y., Li, M., Zhou, M., Yang, K., Mao, L., 2013. Quantitative analysis of the waterline method for topographical mapping of tidal flats: a case study in the Dongsha sandbank, China. Remote Sens. 5 (11), 6138–6158.

Liu, J.G., Mason, P.J., 2016. Image Processing and GIS for Remote Sensing: Techniques and Applications. John Wiley & Sons.

Mahar, G.A., 2010. Geomorphic Degradation of Indus Delta and its Demographic Impact. Doctoral dissertation. University of Karachi, Karachi.

Masood, H., Afsar, S., Zamir, U.B., Kazmi, J.H., January, 2015. Application of comparative remote sensing techniques for monitoring mangroves in Indus Delta, Sindh, Pakistan. Biol. Forum 7 (1), 783.

Mitsch, W.J., Gosselink, J.G., 2000. The value of wetlands: importance of scale and landscape setting. Ecol. Econ. 35 (1), 25–33.

Mokarram, M., Roshan, G., Negahban, S., 2015. Landform classification using topography position index (case study: salt dome of Korsia-Darab plain, Iran). Model. Earth Syst. Environ. 1 (4), 40.

National Institute of Oceanography, Pakistan, Hydraulic Monitoring of Tidal Link Drain (LBOD), First Annual Progress Report (1995).

NIO, 1995. Hydraulic monitoring of tidal link drain (LBOD) Revised April 1996. Natl. Inst. Oceanogr. 1–20.

Parekh, A., Gnanaseelan, C., Deepa, J.S., Karmakar, A., Chowdary, J.S., 2017. Sea Level Variability and Trends in the North Indian Ocean. In Observed Climate Variability and Change over the Indian Region, pp. 181–192.

Rahman, M.U., 1960. Irrigation and Field Patterns in the Indus Delta. Ph.D. dissertation submitted. Louisiana State University and Agricultural & Mechanical College. http://digitalcommons.lsu.edu/cgi/viewcontent.cgi?article=1600&context=gradschool_disstheses. (Accessed 27 September 2017).

Richards, J.A., Jia, X., 2006. Remote Sensing Digital Image Analysis: an Introduction. Springer, Berlin.

Ryu, J.-H., Kim, C.-H., Lee, Y.-K., Won, J.-S., Chun, S.-S., Lee, S., 2008. Detecting the intertidal morphologic change using satellite data. Estuar. Coast. Shelf Sci. 78, 623–632.

Saleem, M., Aftab, J., Kahkashan, S., Kalhoro, N.A., Ahmad, W., 2014. Diurnal variation of nutrients, water quality and plankton composition in the hajamro creek (indus delta) during north east monsoon period. Nucleus 51 (1), 51–61.

Sarmiento, G.R., Cipolletti, M.P., Perillo, M.M., Delrieux, C.A., Perillo, G.M., 2016. Methodology for classification of geographical features with remote sensing images: application to tidal flats. Geomorphology 257, 10–22.
Savenije, H.H.G., 2005. Salinity and Tides in Alluvial Estuaries. Elsevier, New York.
Savenije, H.H.G., 2015. Prediction in ungauged estuaries: an integrated theory. Water Resour. Res. 51, 2464–2476. https://doi.org/10.1002/2015WR016936.
Shroder Jr., J.F. (Ed.), 2002. Himalaya to the Sea: Geology, Geomorphology and the Quaternary. Routledge.
SIDA, 2013. Regional Plan for the Left Bank of River Indus, Delta and Coastal Zone, vol. 1. The Louise Berger Group Inc. and Indus Associated Consultant (Pvt) Ltd.. Main Report.
Spencer, T., Schuerch, M., Nicholls, R.J., Hinkel, J., Lincke, D., Vafeidis, A.T., Brown, S., 2016. Global coastal wetland change under sea-level rise and related stresses: the DIVA Wetland Change Model. Glob. Planet. Change 139, 15–30.
Stive, M.J.F., Wang, Z.B., 2003. Morphodynamic Modelling of Tidal Basins and Coastal Inlets. Chapter-13. In: Advances in Coastal Modelling. Elsevier Science, New York, pp. 367–392.
Syvitski, J.P., Kettner, A.J., Overeem, I., Giosan, L., Brakenridge, G.R., Hannon, M., Bilham, R., 2013. Anthropocene metamorphosis of the Indus Delta and lower floodplain. Anthropocene 3, 24–35.
Tabrez, A.R., Inam, A., Rabbani, M.M., Clift, P., Giosan, L., Danish, M., 2013. An Assessment of Sediment and Carbon Fluxes to the Indus Delta. A report by National Institute of Oceanography, Pakistan. https://www.researchgate.net/profile/Asif_Inam/publication/235721908_An_Assessment_of_Sediment_and_Carbon_Fluxes_to_the_Indus_Delta/links/0912f512e0d64475d1000000.pdf. (Accessed 28 September 2017).
Tambroni, N., Luchi, R., Seminara, G., 2017. Can tide dominance be inferred from the point bar pattern of tidal meandering channels? J. Geophys. Res. Earth Surf. 122 (2), 492–512.
UNEP-DHI and UNEP, 2016. Transboundary River Basins: Status and Trends. United Nations Environment Programme (UNEP), Nairobi.
Waheed-uz-Zaman, M., Saif, N., 2014. To study feasibility of the generation of tidal power energy at Pakistan creek areas. J. Am. Sci. 10 (10).
Wang, Y., Bonynge, G., Nugranad, J., Traber, M., Ngusaru, A., Tobey, J., Makota, V., 2003. Remote sensing of mangrove change along the Tanzania coast. Mar. Geod. 26 (1–2), 35–48.
WAPDA, 1966. Lower Indus Report, the Atlas. Hunting Technical Services and Sir Mac Donald and Partners.
Weiss, A., 2001. Topographic position and landforms analysis. In: Poster Presentation, ESRI User Conference, San Diego, CA, vol. 200.
Woodworth, P., Foden, P., Pugh, J., Mathews, A., Aarup, T., Aman, A., Ashraf, M., 2009. Insight into long term sea level change based on new tide gauge installations at Takoradi, Aden and Karachi. Int. Hydrogr. Rev. (1)